

Enhancement of the critical current density by increasing the collective pinning energy in heavy ion irradiated Co-doped BaFe₂As₂ single crystals

N. Haberkorn,¹ Jeehoon Kim,² K. Gofryk,³ F. Ronning,³ A. S. Sefat,⁴

L. Fang,⁵ U. Welp,⁵ W. K. Kwok,⁵ and L. Civale.³

¹ *Centro Atómico Bariloche, Bariloche, 8400, Argentina.*

² *CALDES, Institute for Basic Science, Pohang, Korea, and Department of Physics, Pohang University of Science and Technology, Pohang, Korea.*

³ *Los Alamos National Laboratory, Los Alamos, NM 87545 USA*

⁴ *Oak Ridge National Laboratory, Oak Ridge, TN 37831, USA*

⁵ *Materials Science Division, Argonne National Laboratory, Argonne, Illinois 60439, USA*

e-mail corresponding author: nhaberk@cab.cnea.gov.ar. Tel : +54 0294 444 5147- FAX: +54 0294 444 5299

Keywords: iron superconductors; vortex dynamics; heavy ion irradiation.

We investigate the effect of heavy ion irradiation (1.4-GeV Pb) on the vortex matter in Ba(Fe_{0.92}Co_{0.08})₂As₂ single crystals by SQUID magnetometry. The defects created by the irradiation are discontinuous amorphous tracks, resulting in an effective track density smaller than 25% of the nominal doses. We observe large increases in the critical current density (J_c), ranging from a factor of ~ 3 at low magnetic fields to a factor of ~ 10 at fields close to 1 T after irradiation with a nominal fluence of $B_\Phi = 3.5$ T. From the normalized flux creep rates (S) and the Maley analysis, we determine that the J_c increase can be mainly attributed to a large increment in the pinning energy, from < 50 K to ≈ 500 K, while the glassy exponent μ changes from ~ 1.5 to < 1 . Although the enhancement of J_c is substantial in the entire temperature range and S is strongly suppressed, the artificial pinning landscape induced by the irradiation does not modify significantly the crossover to fast creep in the field-temperature vortex phase diagram.

1. Introduction

The discovery of iron based superconductors¹ in 2008 has allowed the study of vortex pinning and dynamics in a large and disparate new group of materials.² The response of a type II superconductor to an applied magnetic field depends³ on the characteristic length scales penetration depth (λ) and coherence length (ξ), the superconducting critical temperature (T_c), and the angular dependence of the energy gap function $\Delta(\mathbf{k})$. The effective range of the pinning force must be of the order of ξ to adequately pin a vortex. Therefore, materials with a short ξ are particularly susceptible to pinning because the vortex can interact with small imperfections of the crystalline structure. The effectiveness of the pinning centers depends on their geometry and density, and on the intrinsic thermal fluctuations of the vortex matter in the material. The strength of the thermal fluctuations in superconductors is quantified through the dimensionless Ginzburg number (Gi) which derives from a comparison of the thermal energy with the condensation energy in the coherence volume, $Gi = \frac{1}{2} \left(\frac{T_c}{H_c^2(0)\epsilon\xi^3(0)} \right)^2$, where $H_c(0) = \frac{\phi}{2\sqrt{2}\xi(0)\lambda(0)}$ is the thermodynamic critical field at zero temperature and ϵ is the anisotropy parameter.³ In conventional low T_c superconductors (LTS), Gi is $\approx 10^{-8}$, which results in very slow vortex dynamics, whereas cuprates such as $\text{YBa}_2\text{Cu}_3\text{O}_{7-\delta}$ (YBCO) have $Gi \approx 10^{-2}$. The large Gi in cuprates manifests in high flux creep rates, phase diagrams that include crossover fields depending on the pinning landscape, and vortex-liquid phases at high temperatures.³ The pnictide superconductors include compounds with intermediate and high thermal fluctuations.^{4,5}

According to the collective creep theory, the dynamics in a glassy vortex phase³ is described by an effective activation energy as a function of current density (J)

$$U_{eff} = \frac{U_0(T)}{\mu} \left[\left(\frac{J}{J_c} \right)^\mu - 1 \right] \quad [1]$$

where $U_0(T) = U_0 G(T)$ is the scale of the pinning energy, U_0 is the collective pinning barrier at $T=0$ in the absence of a driving force, $G(T)$ contains the temperature (T) dependence of the superconducting parameters, and μ is the regime-dependent glassy exponent determined by the bundle size and vortex lattice elasticity. Based on the model of the nucleation of vortex loops, for random point defects in the three-dimensional case, μ is 1/7, 3/2 or 5/2, and 7/9 for single vortex, small-bundle and large-bundle creep, respectively.³ Experimental studies on YBCO show a gradual evolution of μ from small to large bundles as H is increased (no discrete values).⁶ From eq. [1], the temperature dependence of the creep rate (S) results in

$$S = -\frac{d(\ln J)}{d(\ln t)} = \frac{T}{U_0 + \mu T \ln(t/t_0)} = \frac{T}{U_0} \left(\frac{J}{J_c} \right)^\mu \quad [2]$$

where t_0 is a vortex hopping attempt time. The $U_{eff}(J)$ can be determined by the so called ‘‘extended Maley analysis’’.⁷ Considering that J decays following the usual thermally activated rate $\frac{dJ}{dt} = -\left(\frac{J_c}{\tau}\right) e^{-\frac{U_{eff}(J)}{T}}$, the final result is $U_{eff}(J, T) = -T \left[\ln \left| \frac{dJ}{dt} \right| - C \right]$, where $C = \ln(J_c/\tau)$ is a nominally constant factor. For an overall analysis it is necessary to consider $G(T)$, which results in $U_{eff}(J, 0) \approx U_{eff}(J, T)/G(T)$.⁸

Among the families of pnictides, one of the most studied is the group of the AFe_2As_2 compounds (122 system), where A is an alkaline-earth.⁹ In particular, the cobalt-doped compounds $Ba(Fe_{1-x}Co_x)_2As_2$ ($0.4 < x < 0.15$) present a wide span of intrinsic superconducting properties depending on x , allowing a broad study of vortex dynamics in the same system. The optimally doped compound ($x=0.08$) has $T_c = 26$ K,⁽¹⁰⁾ $\lambda_{ab}(0) = 260$ nm,⁽¹¹⁾ $\xi_{ab}(0) = 2.6$ nm,⁽¹²⁾ and depairing current density $J_0(T=0) = cH_c / 3\sqrt{6}\pi\lambda \approx 57$ MAcm⁻² (c is the speed of light). The T dependences of $\lambda_{ab}(T)$ and $\xi_{ab}(T)$ are anomalous¹³ and the upper critical field anisotropy decreases from $\gamma_{T \rightarrow T_c} = \frac{H_{c2}^c}{H_{c2}^{ab}} \approx 2$ to

$$\gamma_{T \rightarrow 0} = \frac{H_{c2}^c}{H_{c2}^{ab}} \approx 1.$$

The pinning landscape in 122 materials affects the H - T vortex phase diagrams in analogous ways as in the cuprates. Pinning sources in as-grown Co-doped $BaFe_2As_2$ single crystals typically include intrinsic pinning,¹⁴ small normal regions,¹⁵ chemical inhomogeneities,¹⁶ and twin boundaries.¹⁷ The 122 compounds have $G_i \approx 10^4$, intermediate between LTS and cuprates,^{4,18} however they present high creep rates (consistent with small U_0) of the same order as those found in YBCO, and a crossover from elastic to plastic creep at a $H_{cr}(T)$ boundary inside the vortex solid phase.^{4, 19} Pinning can also be artificially introduced by particle irradiation.^{18,20,21} Proton irradiation generates random point defects and produces an increment of J_c and significant changes in the vortex dynamics at low and intermediate temperatures, and its influence is greater in 122 systems with short ξ .²² The increment in J_c can be associated with a reduction in $S(H, T)$ and an enhancement in U_0 .²³ Heavy ion irradiation (columnar defects, CD) also modifies the creep rates even at temperatures close to T_c .²² The influence of heavy ion irradiation has been studied also in other 122 systems such as $Ba_{0.6}K_{0.4}Fe_2As_2$, where remarkable retention of J_c in high-magnetic fields has been reported.²⁴ The similitudes between the vortex physics in cuprates and iron-based superconductors offer the possibility to investigate systematically the relationship between the artificially designed pinning landscapes on the resulting properties. Determining the influence of the pinning landscape on the H - T vortex phase diagram and on parameters such as J_c , U_0 and μ is relevant from both the basic²⁵ and technological points of view.²⁶

In this work we analyze the vortex dynamics and the $J_c(H, T)$ in a pristine and heavy ion irradiated $Ba(Fe_{0.92}Co_{0.08})_2As_2$ single crystal. An annealed $Ba(Fe_{0.92}Co_{0.08})_2As_2$ single crystal was successively irradiated along the c axis with 1.4-GeV Pb-ions to fluences N corresponding to dose-matching fields of $B_\phi = 1$ and 3.5 T ($B_\phi =$

$N\Phi_0$, where $\Phi_0 = 2.07 \times 10^{15} \text{ Tm}^2$ is the flux quantum). A previous study by scanning transmission electron microscopy (STEM) in $\text{Ba}_{0.6}\text{K}_{0.4}\text{Fe}_2\text{As}_2$ single crystals shows that this irradiation produces segmented amorphous tracks with average diameter of 3.7 nm with a density of $\approx 35\%$ of the nominal doses.²⁴ Our results show that the J_c values are systematically increased with the irradiations. The extension of the single vortex pinning regime³ and a peak in the $J_c(H)$ dependences at low temperatures indicate that also in our case the density of tracks is much smaller than the nominal doses ($< 25\%$). The $J_c(H)$ dependences in the pristine sample can be analyzed as the contribution of two types of pinning centers. At low field $J_c(H)$ is dominated by a combination of random and strong pinning centers. As H increases, localized regions with weaker superconductivity turn normal, becoming extra pinning centers and causing a second peak in the magnetization. The irradiations with heavy ions enhance J_c and the vortex dynamics becomes dominated by the artificially generated pinning landscape (no features of the second peak in the magnetization remains). In comparison with the unirradiated sample, $J_c(H)$ for the high irradiation fluence shows an increment of ≈ 3 times at low H and a remarkable retention of J_c in high magnetic fields (10 times at 5 K and 1 T). Maley analyses⁷ were performed in the pristine and in the irradiated single crystal. The U_0 values systematically change from < 50 K to ≈ 300 K and ≈ 500 K after the two successive irradiations, whereas μ changes gradually from ≈ 1.5 to ≈ 0.7 . Both extremes are inside of the range predicted by the collective theory for small and large bundles in pinning by random point defects.

2. Experimental

The $\text{Ba}(\text{Fe}_{0.86}\text{Co}_{0.14})_2\text{As}_2$ single crystals used in this study were grown by the FeAs/CoAs self-flux method.²⁷ Initially, the magnetic measurements were performed on a pristine (P-SC) and a post-annealed single crystal¹¹ (AN-SC). As we discuss below, the thermal annealing produces a slight increment on T_c and also modifies the extension of the $J_c(H)$ regimes below the elastic to plastic crossover. No significant changes are produced by the thermal annealing in self-field $J_c(5 \text{ K}, H=0) \approx 0.7 \text{ MA cm}^{-2}$, which are close to reported values in single crystals with similar doping.^{4,18} Afterwards, AN-SC was successively irradiated at the ATLAS facility at Argonne National Laboratory with 1.4-GeV Pb-ions to fluences N corresponding to dose-matching fields of $B_\phi = 1 \text{ T}$ (first time, IRR-1) and 2.5 T (second time; total $B_\phi = 3.5 \text{ T}$, IRR-3.5) along the crystal c -axis.

The magnetization (\mathbf{M}) measurements were performed using a Quantum Design MPMS-7 setup equipped with a superconducting quantum interference device (SQUID) magnetometer. The magnetic field (\mathbf{H}) was applied parallel to the c axis of the single crystal (\mathbf{H}/c). The critical current densities were estimated by applying the Bean critical-state model to the magnetization data obtained in hysteresis loops, which is expressed as $J_c = \frac{20\Delta M}{tw^2\left(l - \frac{w}{3}\right)}$, where ΔM is the difference in magnetization between the top and bottom branches of the hysteresis loop, and t (0.05 mm),

w (0.8 mm), and l (1.3 mm) are the thickness, width, and length of the sample ($l > w$), respectively. The flux creep rates, $S = -\frac{d(\ln J_c)}{d(\ln t)}$, were recorded over periods of one hour. The initial time was adjusted considering the best correlation factor in the log-log fitting of the $J_c(t)$ dependence. The initial critical state for each creep measurement was generated by applying a field of $H \sim 4H^*$, where H^* is the field for the full-flux penetration.²⁸

3. Results and discussion

The T_c of the single crystals was determined from magnetization vs. temperature, resulting in $T_c = 25$ K (P-SC), 26 K (AN-SC), 25.8 K (IRR-1) and 25 K (IRR-3.5). The changes in the T_c by irradiation are smaller than those produced by proton irradiation with a similar increment of $J_c(H \rightarrow 0)$ at low temperatures (see discussion below).^{18,}
²⁹ Figure 1 shows a comparison between $J_c(H)$ at 5 K in P-SC, AN-SC, IRR-1 and IRR-3.5. The unirradiated samples show three clearly different regimes: (I) the low-field regime ($B < B^*$), which can be associated with single vortex pinning³ but can also be affected by self-field effects and geometrical barriers;³⁰ (II) a power-law regime, $J_c \propto H^{-\alpha}$, which can be associated with strong pinning centers;³¹ (III) a fishtail or second peak in the magnetization related with magnetic-field induced pinning. As we discuss below, at high temperatures a fourth regime (IV) appears that can be associated with plastic creep.³² The $J_c(H \rightarrow 0)$ values for both unirradiated samples are the same (≈ 0.75 MAcm⁻²). The main differences between P-SC and AN-SC appear in the regimes (II) and (III), which correspond to the ranges where the power law and the second peak in the magnetization appear. This fact indicates that thermal annealing may produce clustering of atoms³³ (reducing inhomogeneities) that slightly improve pinning at intermediate fields (small change in the α exponent).³¹ Thermal annealing reducing the second peak in the magnetization or fishtail has been also observed in YBCO single crystals.³⁴ The irradiation produces an enhancement in the $J_c(H \rightarrow 0)$ values at 5 K from 0.75 MAcm⁻² to 1.3 MAcm⁻² (IRR-1) and to 2.1 MAcm⁻² (IRR-3.5). Also, there are remarkable differences in $J_c(H)$ dependences between unirradiated and irradiated samples at intermediate and high magnetic fields. For example, J_c at $\mu_0 H = 1$ T in IRR-3.5 is 10 times larger than in the unirradiated samples. This fact can be attributed to correlated disorder, which produces better retention of $J_c(H)$ with \mathbf{H}/c -axis.³⁵ Another important difference that appears in the irradiated sample is the extension of the first regime discussed above. In samples with correlated disorder, the crossover between the regimes I and II (B^*) is related to the matching field.³ The increase in B^* for the irradiated samples is larger (by a factor between 2 and 3) than that expected from self-field^{36,37} or geometrical barriers by considering the increment in J_c . This means that B^* after irradiation really indicates the end of the single vortex pinning and that this regime has been extended according with the expectations for pinning by CD. However, the B^* values (see fig. 1) are in both cases much smaller than the nominal B_ϕ . This fact can be associated with both the low effectiveness of the irradiation²⁴ and the

small diameter of the discontinuous tracks.³ It is important to note that a small shoulder (J_c^{MAX}) appears in the $J_c(H)$ dependences at $\mu_0 H < B^*$. These maxima in $J_c(H)$, which occur at ≈ 0.13 T and ≈ 0.75 T for IRR-1 and IRR-3.5 respectively, may indicate a pseudo matching field generated by the discontinuous linear tracks. The concept of Mott insulator corresponds to a vortex density in which every columnar defect is occupied by a single vortex line (B_ϕ) and half-loop excitations between neighbor tracks are avoided.³ Ideally, B_ϕ is the crossover between two different vortex regimes; a single vortex regime ($\mu_0 H < B_\phi$) with dominant vortex-defects interactions and a plastic regime ($\mu_0 H > B_\phi$) with different dynamics for the vortices that exceed B_ϕ .³ However, experimentally the vortex dynamics at $\mu_0 H > B_\phi$ depends on the effectiveness of the pinning by defects between the tracks (random point or strong), and the temperature (thermal depinning).³⁸ In agreement with that, at $\mu_0 H > B^*$ the irradiated samples present a power law dependence similar to those present in the P-SC and AN- SC ($\alpha \approx 0.55$). The increment of the temperature renormalizes the single-vortex pinning potential energy by thermal fluctuations.

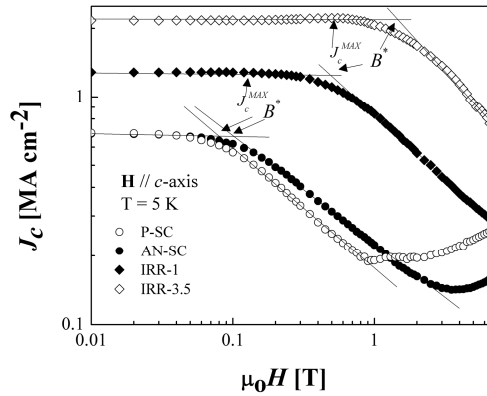


Figure 1. Critical current density J_c at $T = 5$ K of P-SC, AN-SC annealed, IRR-1 and IRR-3.5 $\text{Ba}(\text{Fe}_{0.86}\text{Co}_{0.14})_2\text{As}_2$ single crystal. Black arrows indicate a small maximum in the J_c values and the crossover between the regimes I and II (B^*).

In order to understand the influence of the defects introduced by the heavy ion irradiation, we performed $J_c(H)$ and $J_c(t)$ studies at different T in AN-SC, IRR-1 and IRR-3.5. Figure 2 shows $J_c(H)$ at six different temperatures ($T = 5$; 10; 15; 20; 22K and 24 K) in AN-SC. The different regimes present in $J_c(H)$ were previously discussed in ref. [18]. The crossover between the regimes and the changes in the pinning potential are manifested as a modulation in $S(H)$.^{4,32} Here we will analyze in detail the regime II. The α exponent decreases as function of temperature between 5 and 10 K, which is opposite to the expectation from thermal depinning assuming that pinning is dominated by the same type of defects.³⁸ Usually similar S are observed for the same α , and both parameters are affected by temperature due to an increment in the vortex-vortex interaction.³⁸ An opposite behavior indicates a change in the dominant pinning mechanism that is also manifested as a modulation in the $S(T)$ (see inset 2b).

Figure 2b shows a Maley analysis for AN-SC at $\mu_0 H = 0.3$ T (at this magnetic field the regime II is present between 5 and 20 K). We combined the $S(T)$ data and the Maley method to extract the J_0 , U_0 and μ values from eqs. (1) and (2). To fit $S(T)$ we used $\ln(t/t_0) \sim 30$,⁽³⁹⁾ and we found that the experimental data in the Maley analysis can be adjusted by using⁸ $G(T) = \left(1 - \left(\frac{T}{T_c}\right)^2\right)^{1.5}$ and considering two different sets of data: $T < 7.5$ K and $9 < T < 20$ K. The obtained values for the low temperature regime are $\mu = 1.36$ (5), $J_0 = 0.60$ (5) MA cm⁻² and $U_0 = 30$ (5) K, while the fit for $T > 9$ K gives $\mu = 1.505$, $J_0 = 0.60$ (0.05) MA cm⁻² and $U_0 = 35$ (10) K. The good agreement between the experimental data and the prediction of eq. 2 indicates that the $S(T)$ modulation in the second regime can be explained by a slight increment in the μ values. The estimated μ values for both temperature ranges are inside the limits predicted for creep of small bundles associated with random point defects. It is important to mention that is not possible to estimate the U_0 and μ values in the regime III by the Maley analysis because the pinning landscape depends on both H and T , which modify significantly the U_0 between successive relaxation curves.

In samples with only random point defects (weak pinning) a collective creep single vortex regime (SVR) with $\mu = 1/7$ is predicted at small magnetic fields below the crossover from SVR to vortex bundles expected at $B_{sb} = \beta_{sb} \frac{J_c}{J_0} H_{c2}$, with $\beta_{sb} \approx 5$.³ However this regime, which should produce a plateau with very large S at high temperatures, $S \sim (\mu \ln(t/t_0))^{-1} \sim 7/30$, is typically not observed except under very particular conditions.³⁹ This is in part because the range of magnetic field where the SVR appears is strongly suppressed by temperature, and in part because there is usually a low density of strong pinning centers that are important at low H . The μ values for the different vortex regimes in mixed pinning landscapes that include a low density of strong pinning centers and random point defects have not been predicted, but it is natural to expect that in this scenario J_c will be larger than the values expected solely for random point defects while the creep rates will be larger than expected solely for strong pinning centers. This effect should be more noticeable at low temperatures where a large field extension of the SVR is expected, in agreement with the gradual reduction of S with increasing T usually observed in Ba(Fe_{1-x}Co_x)₂As₂ single crystals at intermediate magnetic fields (inside of the power law regime).^{4,18}

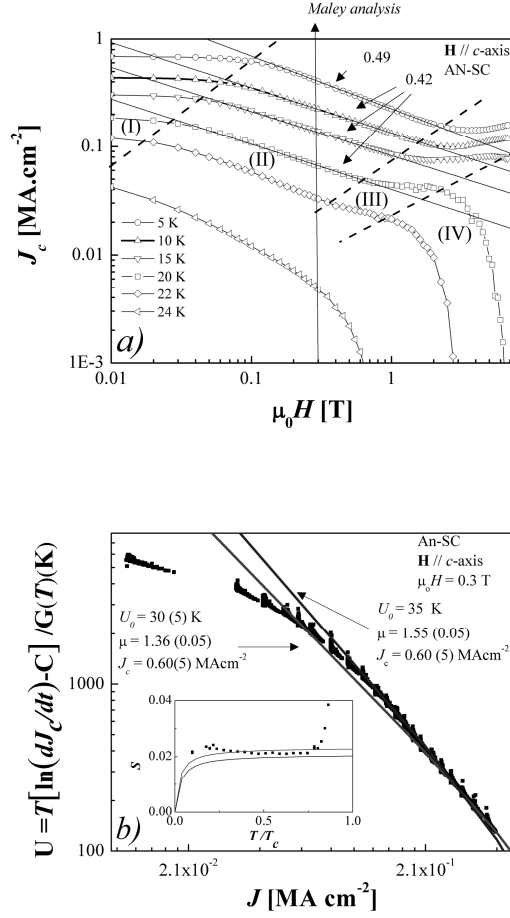


Figure 2. a) J_c vs H dependence with $\mathbf{H} \parallel c$ -axis at different temperatures (5, 10, 15, 20, 22 and 24 K) in the annealed $\text{Ba}(\text{Fe}_{0.82}\text{Co}_{0.18})_2\text{As}_2$ single crystal. b) Maley analysis of AN-SC with $\mu_0 H = 0.3\text{T}$ with $C = 13$. Inset: Temperature dependence of the creep relaxation rate $S(T)$ with $\mu_0 H = 0.3\text{T}$. The $S(T)$ dependence considering eq. 2 is also included.

Figure 3 a. shows J_c vs H in IRR-1 and IRR-3.5 at several temperatures (5 K, 10 K and 20 K). The comparison between the $J_c(H)$ dependences of AN-SC and the irradiated samples shows that the regime III disappears (or is masked) in all the range of temperature. On the other hand, the single vortex state ($\mu_0 H < B^*$) is strongly reduced between 10 and 20 K and the α exponent (related to the regime II) is not evident at 20 K. Both facts can be associated with a reduction of the pinning produced by discontinuous tracks by the $\xi(T)$ evolution and thermal fluctuations. As we mention above, the 1.4-GeV Pb-ions in an isostructural material produce discontinuous tracks with diameter average of 3.7 nm.²⁴ A crossover from a strong pinning regime at low T to weaker pinning at high T is expected when $\sqrt{2}\xi(T) = r_d$ (with $\xi(T) = \xi(0)(1-T/T_c)^{1/2}$) at a temperature T_{cr} defined by $\frac{T_{cr}}{T_c} = 1 - \frac{2\xi^2(0)}{r_d^2}$.

According to that, the $\xi(T)$ dependence modifies the scales for the pinning and most of the defects generated by the irradiation (even the larger ones) are in the limit of weak pinning centers at $T > 15$ K (pinning by reduction of the order parameter).³ The Gaussian distribution in the tracks diameter makes it impossible to distinguish between a crossover associated with the $\xi(T)/r_d$ ratio and thermally activated depinning.³ The smooth $J_c(H)$ dependence at 20 K in IRR-3.5 can be associated with the presence of big defects generated by the two successive irradiations (vortices remain inside the discontinuous tracks). Figure 3b shows Maley analyses at three different H (0.1 T, 0.3 T and 1 T) in IRR-1. The inset in the figure 3b corresponds to the $S(T)$ dependences at the same H . The $S(T)$ values are smaller than in AN-SC. By combining the Maley analysis and the $S(T)$ the obtained values are: $\mu = 1.36$ (0.05), $J_0 = 1.6$ (1) MA cm⁻² and $U_0 = 280$ (30) K at 0.1 T; $\mu = 1.2$ (0.1), $J_0 = 1.6$ (0.1) MA cm⁻² and $U_0 = 300$ (20) K at 0.3 T; and $\mu = 1.03$ (0.05), $J_0 = 1.2$ (0.1) MA cm⁻² and $U_0 = 320$ (20) K at 1 T. For all H , the irradiation produces a large increase in U_0 and a small reduction in the μ exponent. Figure 3c shows Maley analyses at the same three fields in IRR-3.5, and the inset shows the corresponding $S(T)$ dependences. Repeating the same fitting procedure we obtain: $\mu = 1.00$ (5), $J_0 = 2.6$ (0.1) MA cm⁻² and $U_0 = 440$ (40) K for 0.1 T; $\mu = 0.80$ (0.07), $J_0 = 2.6$ (0.1) MA cm⁻² and $U_0 = 580$ (80) K for 0.3 T; and $\mu = 0.72$ (0.05), $J_0 = 2.5$ (0.1) MA cm⁻² and $U_0 = 560$ (40) K for 1 T. In conclusion, the increment in $J_c(H)$ produced by the irradiation is due to a strong increment of the U_0 values, whereas the μ exponent changes gradually from 1.5 to < 1 . The summary of the obtained parameters is presented in table 1.

Sample	Doses $B\phi$ [T]	T_c [K]	J_c (5 K, H = 0) [MA cm ²]	U_0 [K]			μ		
				0.1 T	0.3 T	1 T	0.1 T	0.3 T	1 T
AN-SC	0	26.0 (0.1)	0.75		30 (5)			1.36 (0.05)	
IRR-1	1 T	25.8 (0.1)	1.3	280(30)	300(20)	320(20)	1.36 (0.05)	1.2 (0.1)	1.03 (0.05)
IRR-3.5	3.5 T	25.0 (0.1)	2.1	440(40)	580(80)	560(40)	1.00 (0.05)	0.80 (0.7)	0.72 (0.05)

Table 1. Summary of 1.4-GeV Pb irradiations: dose, superconducting critical temperature (T_c) obtained from magnetization, critical current density at self-field and 5 K, collective pinning barrier (U_0) and the glassy exponent (μ) for several applied magnetic fields.

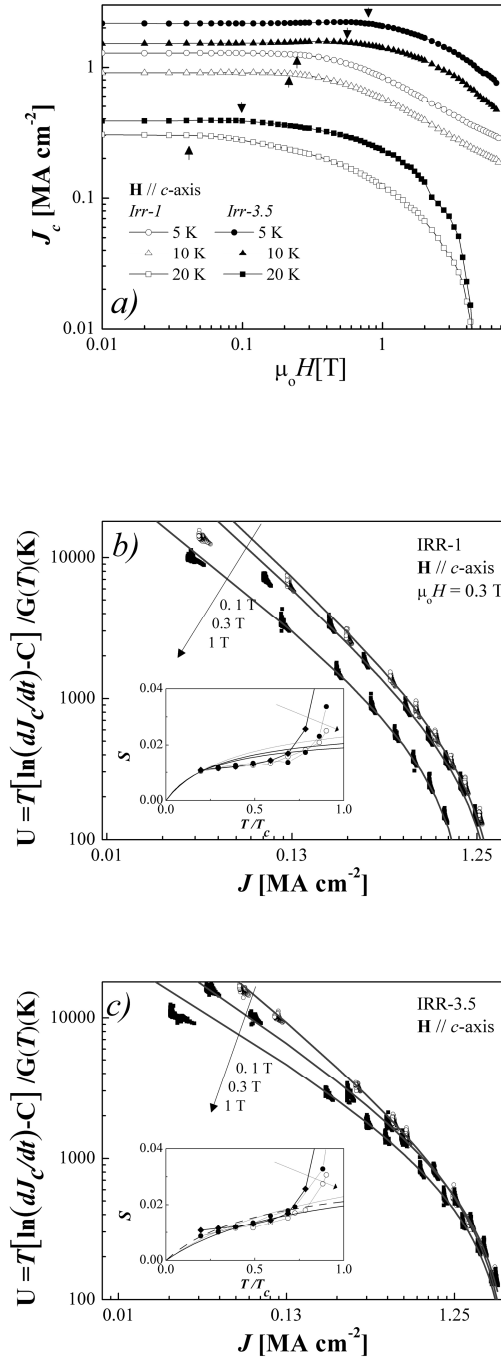
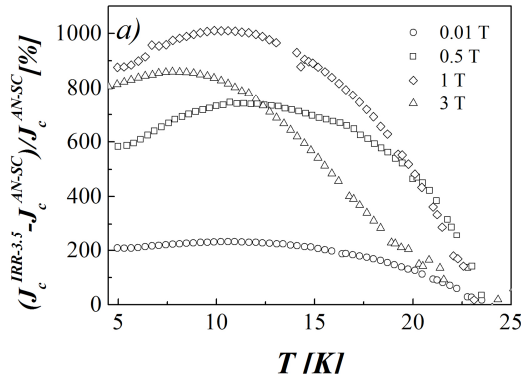


Figure 3) a) J_c vs H dependence with $\mathbf{H} // c$ axis at different temperatures (5, 10, and 20 K) in IRR-1 and IRR-3.5. Arrows indicate B^* . b) Maley analyses of IRR-1 with $\mu_0 H = 0.1$ T, 0.3 T and 1 T. c) Maley analyses of IRR-3.5 with $\mu_0 H = 0.1$ T, 0.3 T and 1 T. The constant $C = 13$ in both cases (all the H). Insets: Temperature dependence of the creep relaxation rate ($S(T)$) at the same H values. $S(T)$ dependence considering eq. 2 is also included.

Figure 4a shows the relative increase in $J_c(T)$ produced by the highest irradiation dose, $((J_c^{\text{IRR-3.5}} - J_c^{\text{AN-SC}})/J_c^{\text{AN-SC}})[\%]$, at several H . The increment of $J_c(H=0)$ at low temperatures in IRR-3.5 are close to those found in proton irradiated single crystals with fluences of $2 \times 10^{16} \text{ cm}^{-2}$.¹⁸ However, heavy ion irradiation enhances $J_c(H)$ in all the range of H and T , the differences being more noticeable close to B^* . The pinning enhancement remains significant up to temperatures close to T_c . Figure 4b shows the relative increase in $J_c(T)$ between the first and second irradiation, $(J_c^{\text{IRR-3.5}} - J_c^{\text{IRR-1}})/J_c^{\text{IRR-1}}[\%]$, at the same fields. The absolute values of $J_c(T)$ are increased in all the range of magnetic fields, but the largest increments are at high H . The mixed pinning landscape generated by both types of irradiations does not modify significantly the J_c values at small field but generate field-independent critical currents in very high fields.³⁷ For comparison, isostructural $(\text{Ba,K})\text{Fe}_2\text{As}_2$ single crystals present similar values of J_c at low temperatures and small fields when they are irradiated with protons²² and heavy ions.²⁴ These facts indicate that the pinning is not strongly affected at small field (low vortex-vortex interaction) but on the other hand the mixed pinning landscape may be very effective at high fields in part due to the high density of random small defects and in part due to synergistic effects with the correlated disorder such as suppression of double-kinks expansion. Similar behavior has been observed in YBCO single crystal irradiated with splayed columnar defects.³⁹



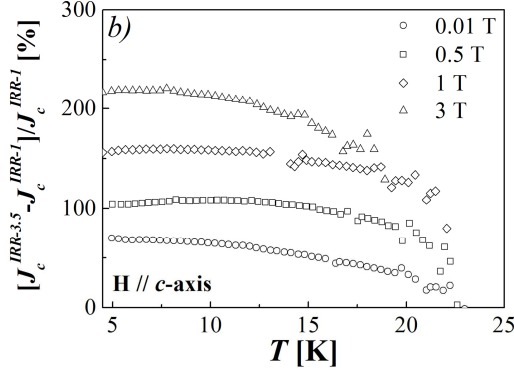


Figure 4. Percentile comparison between the evolution of the $J_c(T)$ dependences at $\mu_0 H = 0.01$ T, 0.5 T, 1 T and 3 T. *a)* $(J_c^{IRR-3.5} - J_c^{AN-SC})/J_c^{AN-SC}$ [%]; *b)* $(J_c^{IRR-3.5} - J_c^{IRR-1})/J_c^{IRR-1}$ [%].

We have previously shown in Ref [18] that proton irradiation enhances J_c over a wide range of temperatures, but does not modify the elastic to plastic crossover in the H - T phase diagram of Co-122 single crystals. Figure 5 shows a comparison between $S(T)$ in AN-SC and IRR-3.5T at $\mu_0 H = 1, 2$ and 3 T. Again we find that, the large increment in the J_c over the whole temperature range notwithstanding, the modification of the pinning landscape produced by the heavy ion irradiation does not alter significantly the elastic to plastic crossover.^{4,18} This fact suggests that the crossover is associated with an intrinsic increment of the thermal fluctuations in the system. The low efficiency of the irradiation and the presence of a wide distribution of track diameters preclude the estimation of a depinning temperature by thermal fluctuations. A more detailed analysis of the resulting J_c and U_0 in samples with large defects such as nanoparticles²⁶ and nanorods³⁵ is necessary to clarify this issue. The increments of J_c (see fig. 4a) are directly related to the reduction of the S values (see fig. 5) by an order of magnitude increment in U_0 . Finally, it is important to note that, although the U_0 and μ exponents in our crystals after irradiation reaches values similar to those observed in YBCO,³ the J_c is significantly lower. The J_c of a superconductor depends on both the pinning energy U_0 of the defects and their density. This suggests that the defect density in our crystals is much lower, implying that further J_c enhancements are still possible in 122 compounds by optimization of the pinning landscape.

4. Conclusions

In summary, we analyze the influence of the pinning landscape created by heavy ion irradiation (discontinuous tracks) on the vortex dynamics of a $\text{Ba}(\text{Fe}_{0.86}\text{Co}_{0.14})_2\text{As}_2$ single crystal. The results can be understood by considering the collective creep theory. A large increase of U_0 (from < 50 K to ≈ 500 K) reduces the vortex creep rates and enhances J_c by factors from around 200% at small magnetic fields to around 1000% at 1 T (at low and intermediate temperatures). The μ exponent progressively changes from ≈ 1.5 to < 1 by the successive irradiations. The increment of the J_c values is pervasive throughout all the H - T range analyzed. It is important to mention that no appreciable changes were observed in the crossover to fast creep (plastic creep), which indicates that larger pinning centers are necessary to reduce creep rates at high temperatures.

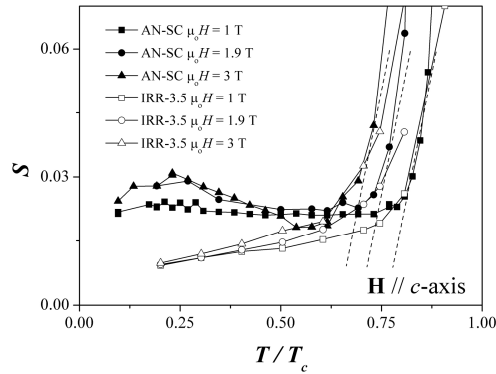


Figure 5. Temperature dependence of the flux creep rate S in AN-SC and IRR-3.5T at $\mu_0 H = 1, 2$ and 3 T.

Acknowledgements

Work at LANL (all magnetometry measurements) and at ORNL (sample preparation and basic characterization) was supported by the US Department of Energy, Office of Basic Energy Sciences, Division of Materials Sciences and Engineering. Work at ANL (irradiation) was supported by the US Department of Energy, Office of Basic Energy Sciences, Division of Materials Sciences and Engineering and by the U.S. Department of Energy, Office of Nuclear Physics. N. H. is member of CONICET (Argentina).

-
- [1] Y Kamihara, T Watanabe, M Hirano, and H Hosono, 2008 *J. Am. Chem. Soc.* **130** 3296 (.
[2] T Tamegai, T Taen, H Yagyuda, Y Tsuchiya, S Mohan, T Taniguchi, Y Nakajima, S Okayasu, M Sasase, H Kitamura, T Murakami, T Kambara, Y Kanai, 2012 *Supercond. Sci. Technol.* **25** 084008.
[3] G Blatter, M V Feigelman, V B Geshkenbein, A I Larkin, and V M Vinokur, 1994 *Rev. Mod. Phys.* **66** 1125.
[4] R Prozorov, N Ni, M A Tanatar, V G Kogan, R T Gordon, C Martin, E C Blomberg, P Prommapan, J Q Yan, S L Bud'ko, and P C Canfield, 2008 *Phys. Rev. B* **78** 224506.
[5] Ni Ni, Jared M. Allred, Benny C Chan, Robert Joseph Cava, 2011 *Proc. Natl. Acad. Sci. USA* **108** E1019.
[6] J R Thompson, Y Sun, D Christen, L Civale, A Marwick, F Holtzberg, 1994 *Phys. Rev. B* **49** 13287.
[7] M P Maley, J O Willis, H Lessure, M E McHenry, 1990 *Phys. Rev. B* **42** 2639.
[8] J G Ossandon, J R Thompson, D K Christen, B C Sales, Y Sun, K W Lay, 1992 *Phys. Rev. B* **46** 3050.
[9] J Paglione, R L Greene, 2010 *Nat. Phys.* **6** 645.
[10] K Gofryk, A B Vorontsov, I Vekhter, A S Sefat, T Imai, E D Bauer, J D Thompson, F Ronning, 2011 *Phys. Rev. B* **83** 064513.

-
- [11] J Kim, *et al.*, 2012 Supercond. Sci. Technol. **25** 112001.
- [12] M Kano, Y Kohama, D Graf, F Balakirev, A S Sefat, M A McGuire, B C Sales, D Mandrus, S W Tozer, 2009 J. Phys. Soc. Japan **78** 84719.
- [13] Oren Ofer, J C Baglo, M D Hossain, R F Kiefl, W N Hardy, A Thaler, H Kim, M A Tanatar, P C Canfield, R Prozorov, G M Luke, E Morenzoni, H Saadaoui, A Suter, T Prokscha, B M Wojek, Z Salman, 2012 Phys. Rev B **85** 060506(R).
- [14] Cornelis J van der Beek, Marcin Konczykowski, Shigeru Kasahara, Takahito Terashima, Ryuji Okazaki, Takasada Shibauchi, Yuji Matsuda, 2010 Phys. Rev. Lett. **105** 267002.
- [15] H Yang, H Luo, Z Wang, H-H Wen, 2008 Appl. Phys. Lett. **93** 142506.
- [16] S Demirdiř, C J van der Beek, Y Fasano, N R Cejas Bolecek, H Pastoriza, D Colson, Rullier-Albenque, 2011 Phys. Rev. B **84** 094517.
- [17] R Prozorov, M A Tanatar, Ni Ni, A Kreyssig, S Nandi, S L Bud'ko, A I Goldman, P C Canfield, 2009 Phys. Rev. B **80** 174517.
- [18] N Haberkorn, B Maiorov, I O Usov, M Weigand, W Hirata, S Miyasaka, S Tajima, N Chikumoto, K Tanabe, L Civale, 2012 Phys. Rev. B **85** 14522.
- [19] B Shen, P Cheng, Z Wang, L Fang, C Ren, L Shan, H-H. Wen, 2010 Phys. Rev. B **81** 014503.
- [20] T Taen, Y Nakajima, T Tamegai, H Kitamura, T Murakami, 2011 Phys. C **471** 784.
- [21] Y Nakajima, Y Tsuchiya, T Taen, T Tamegai, S Okayasu, M Sasase, 2009 Phys. Rev. B **80** 012510.
- [22] Toshihiro Taen, Takahiro Ohori, Fumiaki Ohtake, Tsuyoshi Tamegai, Kunihiko Kihou, Shige-yuki Ishida, Hiroshi Eisaki, Hisashi Kitamura, 2013 Phys. C **494** 106.
- [23] N Haberkorn, Jeehoon Kim, B Maiorov, I Usov, G F Chen, W Yu, L Civale, 2014 Supercond. Sci. Technol. **27** 095004.
- [24] L Fang, Y Jia, C Chaparro, G Sheet, H Claus, M A Kirk, A E Koshelev, U Welp, G W Crabtree, W K Kwok, S Zhu, H F Hu, J M Zuo, H-H. Wen, and B Shen, 2012 Appl. Phys. Lett **101** 012601.
- [25] A E Koshelev, A B Kolton. 2011 Phys. Rev B **84**, 104528.
- [26] Masashi Miura, Boris Maiorov, Takeharu Kato, Takashi Shimode, Keisuke Wada, Seiji Adachi, Keiichi Tanabe, 2013. Nat. Comm. **4** 2499 (doi:10.1038/ncomms3499)
- [27] A S Sefat, R Y Jin, M A McGuire, B C Sales, D J Singh, and D Mandrus, 2008 Phys. Rev. Lett. **101** 117004.
- [28] Y Yeshurun, A P Malozemoff, A Shaulov, 1996 Rev. Mod. Phys. **68** 911.
- [29] Yasuyuki Nakajima, Toshihiro Taen, Yuji Tsuchiya, Tsuyoshi Tamegai, Hisashi Kitamura, and Takeshi Murakami, 2010 Phys. Rev. B **82** 220504(R).
- [30] D Daeumling and D C Larbalastier, 1989 Phys. Rev. B **40** 9350; L W Conner and A P Malozemoff, 1991 *ibid.* **43** 402.
- [31] C J van der Beek, M Konczykowski, A Abal'oshev, I Abal'osheva, P Gierlowski, S J Lewandowski, M V Indenbom, S Barbanera, 2002 Phys. Rev. B **66** 024523.
- [32] Y Abulafia, A Shaulov, Y Wolfus, R Prozorov, L Burlachkov, Y Yeshurun, D Majer, E Zeldov, H Wühl, V B Geshkenbein, and V M Vinokur, 1996 Phys. Rev. Lett. **77** 1596.
- [33] A O Ijaduola, C Cantoni, M Mitchell, A S Sefat, (unpublished).
- [34] Akihiro Oka, Satoshi Koyama, Teruo Izumi, Yuh Shiohara, Junko Shibata, Tsukasa Hirayama, 2000. Jpn. J. Appl. Phys. **39** 5822.
- [35] B Maiorov, T Katase, I O Usov, M Weigand, L Civale, H Hiramatsu, H Hosono, 2012 Phys. Rev. B **86** 094513.
- [36] N Haberkorn, M Miura, B Maiorov, G F Chen, W Yu, L Civale, 2011 Phys. Rev. B **84** 094522.
- [37] K J Kihlstrom, L Fang, Y Jia, B Shen, A E Koshelev, U Welp, G W Crabtree, W -K. Kwok, A Kayani, S F Zhu and H -H. Wen, 2013 Appl. Phys. Lett. **103** 202601.
- [38] N Haberkorn, M Miura, J Baca, B Maiorov, I Usov, P Dowden, S R Foltyn, T G Holesinger, J O Willis, K R Marken, T Izumi, Y Shiohara, L Civale, 2012 Phys. Rev. B **85** 174504.
- [39] L Civale, L Krusin-Elbaum, J R Thompson, F Holtzberg, 1994 Phys. Rev B **50** 7188.